

THERMAL RECOVERY FROM A MULTIPLE STIMULATED HDR RESERVOIR

DEREK ELSWORTH*

Department of Mineral Engineering, Pennsylvania State University, University Park, Pennsylvania 16802,
U.S.A.

(Received September 1988; accepted June 1989)

Abstract—A conceptual model is presented to describe thermal recovery from an infinite geological body through an arbitrary number of spherical production zones. The dimensionless parameters of volume averaged fluid recovery temperature (\bar{T}_D), fluid circulation rate (Q_D), thermal porosity (Φ_D) and geometry uniquely define response within dimensionless time (t_D). Dimensionless circulation rate (Q_D) is directly proportional to fluid circulation rate and inversely proportional to the radii of the stimulated zones. Histories of thermal recovery are specifically presented for colinear arrays of stimulated zones produced at uniform fluid circulation rates. In the steady condition, mean recovery temperature (\bar{T}_D) is defined purely in terms of dimensionless circulation rates (Q_D) and the relative production geometry. In steady production, the mean output temperature (\bar{T}_D) reduces with an increase in the number of zones as a natural consequence of thermal interference. In the transient case also, production temperature (\bar{T}_D) for multiple zones reduces as both the number of zones and their mutual proximity increases. These consequences are, significantly, apparent for intermediate values of circulation rate (Q_D) only.

NOMENCLATURE

General (All quantities in SI units)

a_i	radius of zone i , m
a_i/s_{ij}	dimensionless separation between influencing zone j and influenced zone i
A_{ij}	components of the thermal conductance matrix, $s^3 \text{ K/kg m}^2$
\bar{A}_{ij}	influence coefficient, dimensionless
B_{ii}	thermal extraction rate of zone i , $\text{kg m}^2/\text{s}^3 \text{ K}$
C_{ii}	volumetric thermal capacity of zone i , $\text{kg m}^2/\text{s}^2 \text{ K}$
k	total number of production zones, integer dimensionless
K_R	thermal conductivity of the rock containing the production zones, $\text{kg m/s}^3 \text{ K}$
ℓ	block dimension, m
m	summation parameter, integer dimensionless
n	current time step of interest, integer dimensionless
q_F	fluid circulation rate within zone i , m^3/s
q_T	thermal flux at zone i , $\text{kg m}^2/\text{s}^3$
Q_D	dimensionless throughput
Q'	modified dimensionless throughput, $Q' = 4\pi/Q_D$
r	radius of interest from origin, m
s_{ij}	separation between the centers of zones i and j , m
s_{io}	separation between influencing zone j and any point on the spherical surface of influenced zone i , m
t	time, s
t^{95}	time to 95% thermal equilibration of rock blocks, s
t_n	current time level of interest, s
t_D	dimensionless time
T_r	temperature at radius r , K
T_D	dimensionless temperature of zone i
\bar{T}_D	mean dimensionless zone temperature
T_i	fluid injection temperature for zone i , K
T_o	fluid outlet temperature for zone i , K

* Formerly at Waterloo Centre for Groundwater Research, University of Waterloo, Waterloo, Ontario, N2L 3G1, Canada.

T_R	<i>in-situ</i> rock temperature, K
Δ	finite differential operator with respect to time, dimensionless
κ	thermal diffusivity of intact rock, m^2/s
ϕ_i	secondary porosity within zone i , dimensionless
Φ_{D_i}	dimensionless secondary porosity of zone i , $\Phi_{D_i} = \rho_S c_S / \rho_R c_R$
$\rho_F c_F$	thermal capacity of fluid circulating in zone i , $kg/m^2 s^2 K$
$\rho_R c_R$	thermal capacity of <i>in-situ</i> rock, $kg/m^2 s^2 K$
$\rho_S c_S$	aggregated thermal capacities of circulatory fluid and rock within zone i , $kg/m^2 s^2 K$
τ	surrogate time used in Duhamel's integral, s
Matrices	
A_{t_m}	matrix of thermal conductance terms at component time level t_m , $s^3 K/kg m^2$
B	matrix of thermal extraction rates, $kg m^2/s^3 K$
C	matrix of volumetric thermal capacities, $kg m^2/s^2 K$
I	identity matrix, dimensionless
q_{T_m}	vector of thermal fluxes at component time level t_m , $kg m^2/s^3$
T_I	vector of fluid inlet temperatures, K
$\langle T_O \rangle_{t_m}$	vector of fluid outlet temperatures at time t_m , K
T_R	vector of initial <i>in-situ</i> rock temperatures, K

INTRODUCTION

Feasibility and longevity calculations for hot dry rock (HDR) geothermal energy schemes have historically been developed through the iterative process of mathematical conjecture and supporting physical verification. Original concepts for thermal recovery within single (Lauwerier, 1955; Carslaw and Jaeger, 1959; Harlow and Pracht, 1972; Abé *et al.*, 1979) and multiple fractured systems (Gringarten and Witherspoon, 1973; Gringarten *et al.*, 1975; Bodvarsson and Tsang, 1982) have been supplemented by the results of field studies, most notably in the U.K. and the U.S. (e.g. Smith, 1975; Murphy, 1982). Current field evidence, gathered most conclusively from the passive seismic record (Pine and Batchelor, 1984; Baria *et al.*, 1987; Fehler, 1987), suggests that reservoir stimulation produces a distinct production zone rather than a single discrete hydraulic fracture. The presence of remnant jointing at depth, together with unfavorably aligned residual shear stresses, are cited as the main factors controlling the development of a distinct stimulated zone.

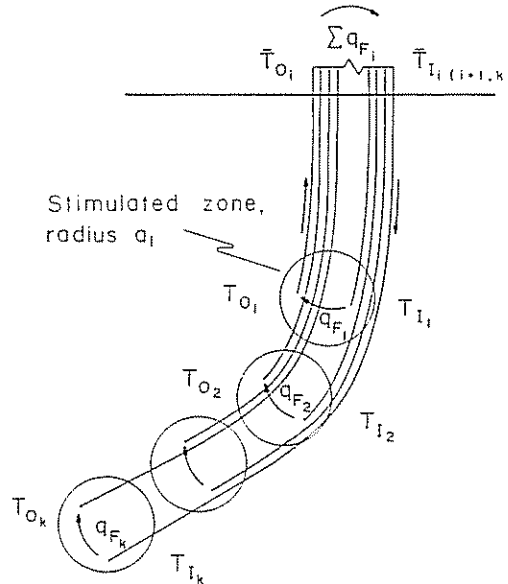


Fig. 1. Schematic of HDR extraction with multiple production zones.

The development of a volumetric zone through downward shearing and penetrated by multiple tortuous flow paths supports the use of thermal recovery mechanisms that are conceptually different from those mentioned above. One such theory has been presented for the withdrawal of thermal energy from a single, spherically stimulated HDR reservoir (Elsworth, 1989a) embedded within a half space. Although use of a single stimulated zone is reasonable in representing the geometries of current experimental HDR schemes, economic viability may reasonably require the development of a multiple stimulated configuration (e.g. Murphy *et al.*, 1985). One potential arrangement may comprise a series of stimulated zones having parallel flow paths as illustrated in Fig. 1. Individual zones may be hydraulically connected or remain unconnected, as conditions dictate, and may be produced at different rates. Assumptions and constraints germane to the conceptual model are presented in the following.

CONCEPTUAL MODEL

Thermal energy is withdrawn from the system through circulation of fluid within a total of k spherical and hydraulically closed stimulated zones of individual radii a_i . The secondary porosity of this artificially stimulated zone is finite with the surrounding medium retaining zero secondary porosity. Fluid is circulated within individual zones at constant volumetric flow rate q_{Fi} with a prescribed injection temperature T_{Ii} and initially unknown outlet temperature T_{O_i} . Further assumptions are made that:

1. Fluid losses associated with temporal pressure changes and void volume increases are assumed negligible over the reservoir lifetime and are neglected. The radii of individual stimulated zones remain static with production. Fluid expansion and buoyancy flow effects are neglected.
2. The temperature of the circulating fluid is raised, immediately upon injection, to the outlet magnitude, T_{Fi} . This requirement necessarily ignores any spatial dependence of fluid temperature within the permeable zone and therefore negates the development of any asymmetric component to the thermal drawdown in the surrounding medium for the case of a single production zone. This assumption is warranted under circumstances where the thermal equilibration of individual rock blocks comprising the permeable zone is rapid, relative to the transit time of the circulating fluid. Where primary interest is the gross (aggregated) magnitude of thermal energy production, rather than point determination of temperature distribution, the assumption is considered reasonable.
3. Thermal equilibrium between the percolating fluid and host rock is maintained at all times within the stimulated zones together with full mixing between the wells. The edge dimensions of individual rock blocks, delineated by active flow paths, are assumed sufficiently small that rapid equilibration will occur. The validity of this assumption may be tested with knowledge of t^{95} , the time to 95% equilibration following a change in surface temperature to any of the individual rock blocks. A spherical idealization of a cubic block, of edge dimension ℓ , yields $t^{95} = 5.9 \times 10^{-2} \ell^2 / \kappa$ where κ is the thermal diffusivity of the rock (Elsworth, 1987) denoted $\kappa = K_R / \rho_R c_R$ with K_R = thermal conductivity and $\rho_R c_R$ = specific heat capacity of the rock.
4. Thermal transport within the stimulated zones is purely advective. Pure conduction is the transport mechanism within the external medium.
5. The thermal capacities of the external rock $\rho_R c_R$, heat exchanging fluid $\rho_F c_F$, and the

saturated stimulated zones $\rho_S c_S$, together with the thermal conductivity of the external rock K_R , remain constant with time.

6. The influence of the natural geothermal gradient over the height of the stimulated zone is assumed negligible. This factor has been illustrated, in previous investigations, to be apparent only at small dimensionless times and is negligible for a realistic range of physical parameters (Gringarten *et al.*, 1975).

7. The domain containing the spherical production zones is infinite.

8. The heat capacity of individual stimulated zones is defined as $\rho_S c_S = (1 - \phi_i)\rho_R c_R + \phi_i \rho_F c_F$, where ϕ_i is the secondary porosity of zone i .

MATHEMATICAL DEVELOPMENT

Consider a total of k spherical production zones within an infinite medium of radii a_i through which fluid is internally circulated at rates q_F , and at inlet and outlet fluid temperatures T_I and T_O , respectively. The global thermal energy balance for the system may be documented as a total of k equations of the form

$$q_T = q_F \rho_F c_F (T_O - T_I)_i + \frac{4}{3} \pi a_i^3 \rho_S c_S \frac{\partial T_O}{\partial t} \quad (1)$$

where q_T is the total thermal flux recovered per unit time from zone i . Equation (1) balances the influent thermal flux with the components extracted through the heat exchanging fluid and the thermal inertia of the centrally stimulated zone.

The radial temperature distribution T_r within an infinite medium, of initial uniform temperature T_R , into which a spherical source of constant strength q_T and radius a_i is initiated at time $t = 0^+$ is recovered as (Carslaw and Jaeger, 1959, p. 248)

$$(T_R - T_r) = \frac{q_T}{4\pi K_R r} \left\{ \operatorname{erfc} \left(\frac{r - a_i}{2(\kappa t)^{1/2}} \right) - \exp \left(\left(\frac{r - a_i}{a_i} \right) + \frac{\kappa t}{a_i^2} \right) \cdot \operatorname{erfc} \left(\left(\frac{r - a_i}{2(\kappa t)^{1/2}} \right) + \left(\frac{\kappa t}{a_i^2} \right)^{1/2} \right) \right\} \quad (2)$$

where r is the radius of interest and κ is the thermal diffusivity of the surrounding solid rock. From this basis, expressions for both the self influence and reciprocal influence of spherical sources may be developed directly.

Self-influence

The uniform temperature change induced at the surface periphery of a spherical source i may be obtained directly from equation (2). Substituting $r = a_i$ and setting $T_r(t) = T_O(t)$ gives

$$\langle T_R - T_O \rangle_i = \frac{q_T}{4\pi K_R a_i} \bar{A}_{ii} \quad (3)$$

where

$$\bar{A}_{ii} = 1 - \exp \left(\frac{\kappa t}{a_i^2} \right) \operatorname{erfc} \left(\frac{\kappa t}{a_i^2} \right)^{1/2} \quad (4)$$

where $\langle T_R - T_O \rangle_i$ represents the area averaged temperature differential at zone i . For self-influence, symmetry dictates that the temperature differential is uniform.

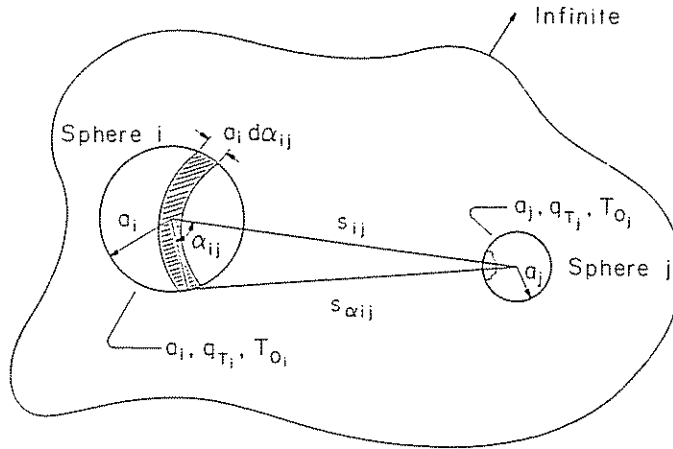


Fig. 2. Relative geometry of spherical production zones within an infinite medium.

Reciprocal influence

The reciprocal influence of a spherical source q_{T_j} upon the temperature distribution over a spherical surface of radius a_i centered a distance s_{ij} distant is illustrated in Fig. 2. The connecting separation $s_{\alpha_{ij}}$ subtended at any angle α_{ij} within the influenced sphere is given by

$$s_{\alpha_{ij}} = s_{ij} \left[1 + \left(\frac{a_i^2}{s_{ij}^2} \right) - \left(\frac{2a_i}{s_{ij}} \right) \cos \alpha_{ij} \right]^{\frac{1}{2}} \quad (5)$$

The areally averaged temperature over the surface of sphere i is, therefore,

$$\langle T_R - T_O \rangle_i = \frac{1}{4\pi a_i^2} \cdot 2\pi a_i^2 \int_0^\pi (T_R - T_r(s_{\alpha_{ij}})) \sin \alpha_{ij} d\alpha_{ij} \quad (6)$$

where $T_r(s_{\alpha_{ij}})$ is the temperature at connecting radius, $s_{\alpha_{ij}}$. Substitution of equation (2) into (6) yields the reciprocal influence of a source centered at j on the averaged temperature distribution at i as

$$\langle T_R - T_O \rangle_i = \frac{q_{T_j}}{4\pi K_R a_j} \bar{A}_{ij} \quad (7)$$

where no summation is implied and

$$\begin{aligned} \bar{A}_{ij} = & \frac{1}{2} \int_0^\pi \frac{a_j}{s_{\alpha_{ij}}} \left\{ \operatorname{erfc} \left(\frac{s_{\alpha_{ij}} - a_j}{2(\kappa t)^{\frac{1}{2}}} \right) - \exp \left(\frac{s_{\alpha_{ij}} - a_j}{a_j} + \frac{\kappa t}{a_j^2} \right) \right. \\ & \left. \times \operatorname{erfc} \left[\left(\frac{s_{\alpha_{ij}} - a_j}{2(\kappa t)^{\frac{1}{2}}} \right) + \frac{(\kappa t)^{\frac{1}{2}}}{a_j} \right] \right\} \sin \alpha_{ij} d\alpha_{ij}. \end{aligned} \quad (8)$$

Where $i = j$, as is the case for self-influence, equation (7) collapses to equation (3).

GLOBAL EQUATIONS

From the principle of linear superposition, the temperature change occasioned at location i

from a total of k sources distributed throughout an infinite medium is given by

$$\langle T_R - T_O \rangle_i = \frac{q_{T_i}}{4\pi K_R a_j} \bar{A}_{ij} \quad (9)$$

where \bar{A}_{ij} and \bar{A}_{ij} are as previously defined and the normal summation convention holds with $j = 1, k$. Equation (9), as written, is for thermal fluxes q_{T_i} that remain constant with time. Duhamel's theorem may be applied to replace the constant fluxes with a condition of linear superposition in time. Equation (9) may be represented in matrix form as

$$\langle T_R - T_O \rangle = A q_T \quad (10)$$

where q_T is a vector of thermal discharges, $\langle T_R - T_O \rangle$ is a vector of temperature differentials and the coefficients of matrix A follow directly from equation (9). Duhamel's theorem allows the thermal flux q_{T_n} at current time t_n to be determined as

$$q_{T_n} = \int_0^{t_n} \frac{\partial}{\partial t} A^{-1} \langle T_R - T_O \rangle d\tau \quad (11)$$

where the coefficients comprising A are modified from the previous by replacing t with $(t - \tau)$. The continuous differential may be replaced in discrete form as

$$q_{T_n} = - \sum_{m=1, n} A_{m,n}^{-1} \Delta \langle T_O \rangle_{t_m} \quad (12)$$

for constant T_R . The component terms of $A_{m,n}$ are represented at the time level t_n as,

$$A_{ij} = \frac{1}{8\pi K_R \Delta t_m} \int_{t_{m-1}}^{t_m} \int_0^\pi \frac{1}{s_{a_j}} \left\{ \operatorname{erfc} \frac{s_{a_j} - a_j}{2(\kappa(t_n - \tau))^{1/2}} - \exp \left[\frac{s_{a_j} - a_j}{a_j} + \frac{\kappa(t_n - \tau)}{a_j^2} \right] \right. \\ \left. \cdot \operatorname{erfc} \left[\frac{s_{a_j} - a_j}{2(\kappa(t_n - \tau))^{1/2}} + \frac{(\kappa(t_n - \tau))^{1/2}}{a_j} \right] \right\} \sin a_{ij} da_{ij} d\tau \quad (13)$$

for $i \neq j$, where

$$\Delta t_m = t_m - t_{m-1} \quad (14a)$$

$$\Delta \langle T_O \rangle_{t_m} = \langle T_O \rangle_{t_m} - \langle T_O \rangle_{t_{m-1}} \quad (14b)$$

and for $i = j$ may be determined separately as

$$A_{ii} = \frac{1}{4\pi K_R a_i \Delta t_m} \int_{t_{m-1}}^{t_m} \left\{ 1 - \exp \frac{(\kappa(t_n - \tau))}{a_i^2} \operatorname{erfc} \frac{(\kappa(t_n - \tau))^{1/2}}{a_i} \right\} d\tau. \quad (15)$$

In matrix notation, the energy balance relationship of equation (1) may be differenced to yield, at current time level t_n

$$q_{T_n} = B \langle T_O - T_I \rangle_{t_n} + \frac{1}{\Delta t_n} C \Delta \langle T_O \rangle_{t_n} \quad (16)$$

where the component diagonal matrixes B and C are invariant with time and are given as

$$B_{ii} = q_F \rho_F c_F; \quad B_{ij} = 0 \quad (i \neq j) \quad (17a)$$

$$C_{ii} = \frac{4}{3} \pi a_i^3 \rho_S c_S; \quad C_{ij} = 0 \quad (i \neq j). \quad (17b)$$

Substituting equation (12) into (16) and rearranging gives the incremental energy balance at time t_n as

$$\left[A_{t_n}^{-1} + B + \frac{1}{\Delta t_n} C \right] \langle T_O \rangle_{t_n} = - \sum_{m=1, n-1} A_{t_m}^{-1} \Delta \langle T_O \rangle_{t_m} + \left[A_{t_n}^{-1} + \frac{1}{\Delta t_n} C \right] \langle T_O \rangle_{t_{n-1}} + B \langle T_I \rangle \quad (18)$$

which may be solved directly for outlet temperatures $\langle T_O \rangle_{t_n}$ at the current time. Of the component matrices, only A_{t_n} is onerous to evaluate, containing an integral in both time and space. The temporal and spatial integrals are evaluated using three and eight point quadrature, respectively. The computational burden is eased somewhat by noting that, for constant time increments (Δt_n), $A_{t_{n-1}}^{-1}$ at time level t_{n-1} is equivalent to $A_{t_n}^{-1}$ at time level t_n .

The dimension of the fully populated interaction matrix A increases in direct proportion to the number of active stimulated zones. The computational effort required to evaluate outlet temperatures at any given time level is, therefore, dependent on both the number of active zones k and the number of preceding temporal iterations n . Exclusive of evaluating the integrals comprising A_{t_n} , the right hand side of equation (18) requires of the order of $nk^2 + k^3$ multiplications at each time level. For a large number of iterations, this effort quickly exceeds that of $\frac{1}{3}k^3 + k^2$ necessary in reducing equation (18) for a known right hand side. If computational advantage is taken of recording the entries of both previously evaluated A matrices and fluid output temperatures $\langle T_O \rangle$, storage requirements are $(k^2 + 1)n$. Of crucial importance, therefore, in determining both computational effort and computational storage requirements are the desired number of time steps.

Dimensionless parameters

Similar to the case for a single stimulated zone, the global equations may be expressed uniquely in terms of a set of dimensionless variables. For k zones, a total of $5k$ dimensionless parameters uniquely describe the performance of the system. Dimensionless output temperatures are regulated by the relationship

$$\frac{\langle T_O - T_I \rangle_i}{(T_R - T_I)_i} = F \left(\frac{q_F \rho_F c_{F_i}}{K_R a_j}, \frac{K_R}{\rho_R c_R a_j^2}, \frac{\rho_S c_{S_i}}{\rho_R c_R}, \frac{a_i}{s_{ij}} \right) \quad (19)$$

where $j = 1, k$ and no summation is implied. In shorthand these quantities are

$$T_{D_i} = F \left(Q_{D_i}, t_{D_i}, \Phi_{D_i}, \frac{a_i}{s_{ij}} \right). \quad (20)$$

Physically, these dimensionless groups may be described as dimensionless output temperature (T_{D_i}), dimensionless reservoir throughput (Q_{D_i}), dimensionless time (t_{D_i}), dimensionless heat capacity or secondary porosity (Φ_{D_i}) and dimensionless zone separation (a_i/s_{ij}).

Dimensional similitude guarantees that systems exhibiting both identical thermal extraction geometries and dimensionless parameter magnitudes Q_{D_i} and Φ_{D_i} will return identical production temperature histories T_{D_i} when viewed relative to dimensionless time t_{D_i} . Since a unique thermal history is recovered for every individual permutation of production geometry, generic graphical representation of thermal histories is infeasible in all but the most simple and geometrically regular instances. In response to this constraint, further discussions are restricted to consideration of a colinear array of production zones.

PARAMETRIC EVALUATIONS AND DISCUSSION

Thermal response to a variety of production scenarios may be conveniently represented in dimensionless form. These provide an extremely powerful method by which reservoir longevity and output may be determined. Predictions may be both qualitative and quantitative. In all instances, a colinear arrangement of producing zones is chosen although, clearly, this is not a limiting facet of the conceptual model. In all cases, dimensionless throughputs (Q_D) and dimensionless time (t_D) are defined with respect to the behavior of one of the component zones. Total system throughput may be recovered as the product of component throughput and the number of zones being produced at that rate.

Steady behavior

In the long term as $(\partial T_O/\partial t) \rightarrow 0$ the energy balance equation may be expressed in matrix format as a direct derivative of equation (18)

$$\langle T_R - T_O \rangle = AB \langle T_O - T_1 \rangle \quad (21)$$

The terms comprising the matrices are determined from equation (8) as $t \rightarrow \infty$ as

$$A_{ii} = \frac{1}{4\pi K_R a_i} \quad (22)$$

$$A_{ij} = \frac{1}{4\pi K_R a_i} \cdot \frac{1}{2} \int_0^\pi \frac{a_i}{s_{a_i}} \sin \alpha_{ij} d\alpha_{ij} = \frac{1}{4\pi K_R a_i} \cdot \frac{a_i}{s_{ij}} \quad (i \neq j) \quad (23)$$

and

$$B_{ii} = q_F \rho_F c_F \quad (24)$$

$$B_{ij} = 0. \quad (i \neq j) \quad (25)$$

The global energy balance relationship of equation (21) may be rearranged to yield

$$\langle T_R \rangle + AB \langle T_1 \rangle = [I + AB] \langle T_O \rangle \quad (26)$$

where I is the identity matrix. In terms of outlet temperatures from each of the stimulated zones, equation (26) may be reordered as

$$\langle T_O - T_1 \rangle = [I + AB]^{-1} \langle T_R - T_1 \rangle. \quad (27)$$

In the case representing a local geothermal gradient of zero where $\langle T_R - T_1 \rangle$ is constant with depth and equal to $(T_R - T_1)$, the steady relation above allows the dimensionless output temperature $\langle T_O - T_1 \rangle_i / (T_R - T_1)$ of the component zones ($i = 1, k$) to be recovered from the sum of terms comprising the i th row of $[I + AB]^{-1}$.

Steady discharge temperatures are controlled by the distribution of dimensionless throughput magnitudes Q_D and the relative production geometry as evidenced through dimensionless separations a_i/s_{ij} . For linear arrangements of production zones, the most likely format in practice, the steady dimensionless output temperatures may be simply evaluated. For constant dimensionless throughput magnitudes Q_D , constant zone dimension a_i and symmetrically uniform separation between centers s_{ij} the output temperatures are, for:

twin zones

$$T_{D1} = Q' \left[1 + Q' + \frac{a}{s_{12}} \right]^{-1} \quad (28)$$

triple zones

$$\begin{bmatrix} T_{D_1} \\ T_{D_2} \end{bmatrix} = Q' \left[\left(1 + Q' + \frac{a}{s_{12}} \right) (1 + Q') - \frac{2a}{s_{12}} \right]^{-1} \begin{bmatrix} 1 + Q' + \frac{a}{s_{12}} \\ 1 + Q' - \frac{2a}{s_{12}} + \frac{a}{s_{13}} \end{bmatrix} \quad (29)$$

and quadruple zones

$$\begin{bmatrix} T_{D_1} \\ T_{D_2} \end{bmatrix} = Q' \left[\left(1 + Q' + \frac{a}{s_{14}} \right) \left(1 + Q' + \frac{a}{s_{12}} \right) - \left(\frac{a}{s_{12}} + \frac{a}{s_{13}} \right)^2 \right]^{-1} \begin{bmatrix} 1 + Q' - \frac{a}{s_{13}} \\ 1 + Q' - \frac{a}{s_{12}} - \frac{a}{s_{13}} + \frac{a}{s_{14}} \end{bmatrix} \quad (30)$$

where subscripts 1 and 2 attached to the dimensionless temperatures refer to outermost and central zones in the linear arrangement, respectively and $Q' = 4\pi/Q_D$. Zones are numbered sequentially 1 through k along the colinear arrangement beginning at one outermost tip. Dimensionless output temperatures may similarly be determined for larger numbers of stimulated zones. For a linear arrangement of contacting equidimensional zones produced at constant rate, the steady dimensionless temperatures are illustrated in Fig. 3.

It is apparent that the average output temperature \bar{T}_D decreases as the number of producing zones increases. The average steady production temperature is a function of geometry and dimensionless throughput Q_D only. Thus, for a ten-fold increase in total throughput, evidenced by transiting either from 1 to 10 zones or from 10 to 100 zones, the steady return of thermal energy is increased less than ten-fold for intermediate values of dimensionless throughput, Q_D . The most favorable energy extraction conditions are for low dimensionless throughput rates representing either low fluid circulation rates or high thermal conductivities of the surrounding rock. Although steady thermal yields at high dimensionless throughputs ($Q_D > 10^2$) increase near proportionately to the increase in number of producing zones, this behavior is clearly far from optimum in all practicality due to the low specific recovery temperature.

As the number of zones in linear arrangement increases, the spread of production temperatures away from the mean value also increases. Production temperatures in the central region of

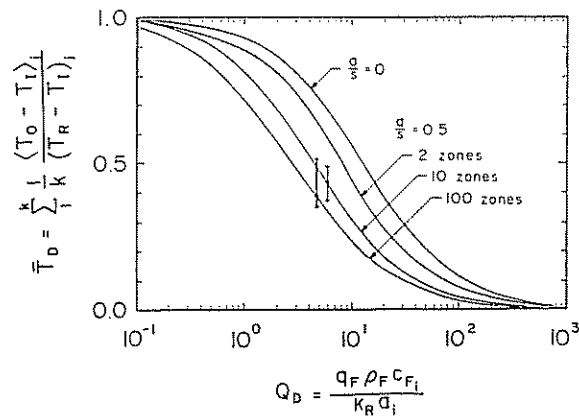


Fig. 3. Average steady state production temperatures (\bar{T}_D) for a colinear, array of equidimensional zones produced at uniform rate. Vertical bar indicates the range of the maximum production temperature span between the central (upper limit) and outermost (lower limit) zones.

the linear arrangement are always the lowest, with the highest temperatures recorded at the extremities. The spread of these production temperatures is available from equations (29) and (30) for triple and quadruple zones and for 10 and 100 zones as evidenced by the spread bar in Fig. 3. With the addition of more zones, the mean output temperature is predominantly influenced by the centrally located production zones.

In the limit as $a/s_{ij} \rightarrow 0$, the results for steady output temperature reduce to

$$T_D = Q'[1 + Q']^{-1} \quad (31)$$

representing the behavior of a single stimulated zone within an infinite body. This behavior presents an upper bound to potential steady production temperatures as evidenced in Fig. 3.

Transient behavior

Solution of equation (18) allows the transient behavior of any multiple stimulated configuration to be determined. For large separations between stimulated zones ($a_i/s_{ij} \rightarrow 0$), the thermal output of the system may be determined exactly from the sum of the components. The broad spacing of the stimulated zones, relative to their radii, precludes mutual interference and thermal histories may be recovered from single production zone solutions as presented elsewhere [Elsworth, 1989a].

The influence of the dimensionless secondary porosity Φ_D in the reasonable range 1.0–1.1 has been illustrated to be insignificant when gauged against the other controlling variables [Elsworth, 1989a]. Results for a single zone, produced at a range of dimensionless throughputs, are illustrated in Fig. 4. Evident from the figure is the presence of bounding behaviors at the extreme values of dimensionless throughput, Q_D . For very large throughputs ($Q_D > 10^4$), output temperatures are fixed in dimensionless time ($t_D Q_D$). This represents the case of minimal thermal replenishment from the surrounding medium and gauges the response of an insulated spherical inclusion only. Small throughputs ($Q_D < 10^{-1}$) precipitate minimal disturbance of the thermal regime surrounding the production zone and thermal output from the system remains near constant with time.

For multiple extraction cases, the results will be most different from the single zone case as $a/s_{ij} \rightarrow 1/2$ for equal sized zones. Results for a linear arrangement are illustrated in Fig. 5. Mean temperatures represented in the figure are obtained by volume averaging outputs from individual zones. Similar to the case of a single zone, threshold behaviors are evident for bounding values of dimensionless throughput, Q_D . For $Q_D > 10^4$ a limiting thermal history in

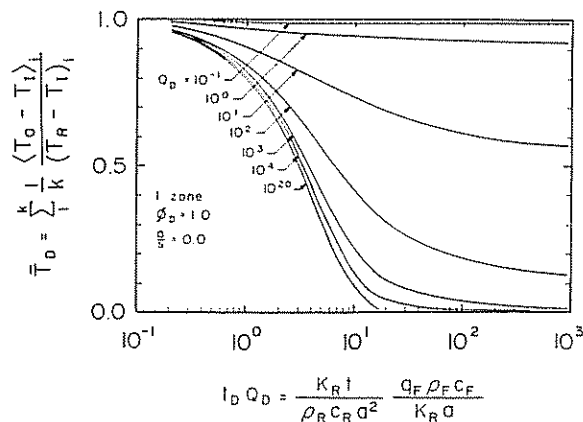


Fig. 4. Variation in dimensionless output temperature (T_D) with dimensionless time (t_D) for a single stimulated zone.

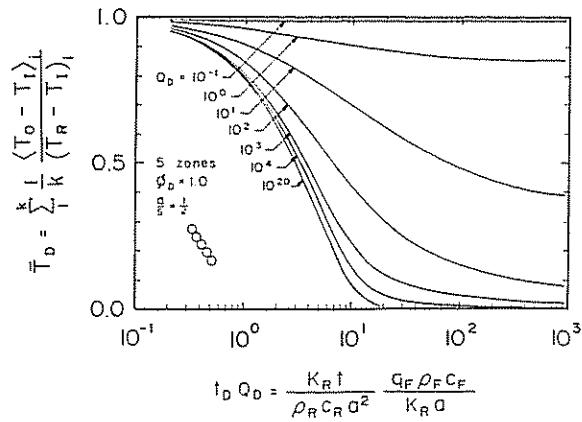


Fig. 5. Variation in the volume averaged dimensionless output temperature (\bar{T}_D) with dimensionless time (t_D) for a five component, colinear array of producing zones.

dimensionless time is apparent and for $Q_D < 10^{-1}$, mean output temperatures remain near constant with time.

For intermediate dimensionless throughputs, $10^{-1} \leq Q_D \leq 10^4$, the mean output temperatures are degraded, over the single case, at dimensionless times $t_D > 10^0$. This is similar to the behavior predicted in the steady case as illustrated in Fig. 3. With an increase in throughput, the degradation occurs at progressively later dimensionless times ($t_D Q_D$) or earlier real times (t). The significance of this degradation, in reality, is therefore conditioned by anticipated useful lifetime of the system. The magnitude of the degradation appears greatest for intermediate magnitudes of dimensionless throughput, $Q_D \approx 10^1$.

Doubling the number of producing zones to ten further degrades relative mean thermal output from the system. Transient results for this case, illustrated in Fig. 6, indicate that the magnitude of degradation is only slightly accentuated over that for five colinear zones. Similar to the previous, this effect is only important for intermediate values of dimensionless throughput ($10^{-1} < Q_D < 10^4$). Also illustrated is the spread of fluid temperatures produced from both the

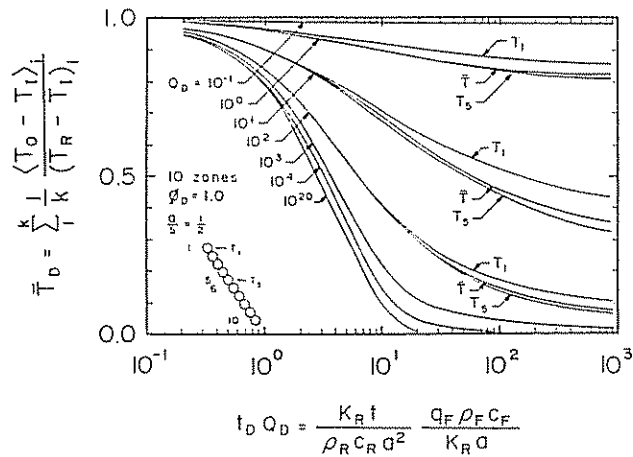


Fig. 6. Variation in the volume averaged dimensionless output temperature (\bar{T}_D) with dimensionless time (t_D) for a ten component, colinear array of producing zones.

innermost and outermost zones in the colinear arrangement. The distinction between the innermost and outermost positions is significant only for the previously designated intermediate range of fluid throughputs. The lowest temperatures of the distribution are returned at the central locations and the highest at the outermost zones. Similar to the single zone case at dimensionless times greater than 10^0 , the discrepancy between central and outermost production temperatures is only significant following this time for multiple arrangements of producing zones. With increasing dimensionless throughput the splitting of temperature histories occurs progressively later.

THERMAL EQUILIBRIUM

The assumption that both rock and percolating fluid remain in thermal equilibrium within the stimulated zone is the most demanding of the model requirements although, beyond radius a , conductive gradients remain permissible. The conditions of this assumption will be approached as fluid throughput rates (q_F) are reduced sufficiently that thermal gradients within the rock comprising the stimulated zone become insignificant. The maximum admissible magnitude of q_F that may be tolerated before the equilibrium assumption is violated may be evaluated by using a thermal drawdown model that accounts for disequilibrium. The parallel fracture model [Gringarten *et al.*, 1975] may be recast using the dimensionless parameters T_D , Q_D , t_D where the scaling length of reservoir radius, a , is replaced by reservoir volume, v , through $v = \frac{4}{3}\pi a^3$. Thus, the equivalent dimensionless parameters become [Elsworth, 1989b]

$$Q_D = \frac{q_F \rho_F c_F}{K_R} \left(\frac{4\pi}{3v} \right)^{1/3} \quad (32)$$

$$t_D = \frac{K_R t}{\rho_R c_R} \left(\frac{4\pi}{3v} \right)^{2/3} \quad (33)$$

with the additional reservoir "shape" factor of $x_E/v^{1/3}$ where $2x_E$ is the separation between adjacent parallel flow channels. In this manner the results of the parallel fracture model, accounting for thermal gradients within the stimulated zone but ignoring heat supply from the external geologic host, may be directly compared with the proposed model.

The individual stimulated volumes of the Los Alamos Fenton Hill reservoir and the Camborne Geothermal Energy Project are of the order of $4 \times 10^6 \text{ m}^3$. Assuming a worst case diffusion length, x_E , separating adjacent flow paths to be of the order of 10 m returns a dimensionless shape factor, $x/v^{1/3}$, of 6.2×10^{-2} . Thermal drawdown for the parallel fracture model is represented in the same semi-log space as the spherical reservoir model for $x/v^{1/3} = 10^{-2}$ in Fig. 7. For small magnitudes of Q_D the parallel fracture model duplicates the assumption of thermal equilibrium between rock and the circulating fluid but does not allow for full mixing. The results for the spherical reservoir model with no external heat supply are also shown. For circulating rates (Q_D) lower than 1.6×10^4 the spherical reservoir model is in reasonable agreement with the parallel fracture model where behavior is bounded as $Q_D \rightarrow 0$. The inability of the spherical model to fit the data for all $Q_D \leq 1.6 \times 10^4$ results from the assumption of full mixing within the stimulated zone being unable to represent the propagation of a thermal wave. However, from the results of Fig. 7, reasonable bounds may be placed on the importance of this inadequacy.

For the chosen magnitude of $x_E/v^{1/3} = 10^{-2}$, the assumption of thermal equilibrium would appear reasonable for $Q_D \leq 1.6 \times 10^4$. Since previous large-scale circulation tests at the Los Alamos reservoir have returned circulation rate magnitudes of the order $Q_D = 10^2$ [Elsworth, 1989a], the threshold Q_D allows for a two order of magnitude increase in circulation rate before

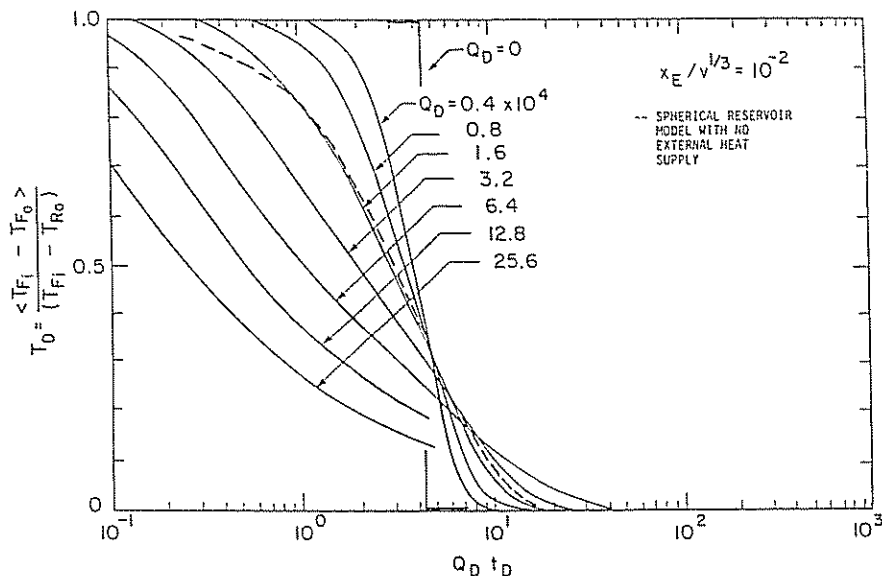


Fig. 7. Variation in dimensionless output temperature (T_D) with dimensionless time (t_D) for the parallel fracture model of geothermal energy extraction.

the assumption of thermal equilibrium is violated. It is suggested, therefore, that the proposed model is broadly applicable to practical problems of HDR geothermal energy recovery.

CONCLUSIONS

For a multiple arrangement of colinear zones, relative thermal output is degraded over the case of a single producing zone. The degradation is apparent only in the sense that doubling the number of zones will less than double the recovery of thermal energy. As the number of zones increases, so does the magnitude of the decrease over the single production case. While this is demonstrated in the previous examples for a contacting colinear arrangement of zones, the effect will become less evident with increased separation. Even for contacting zones, the degraded production is only significant for intermediate magnitudes of dimensionless throughput ($10^{-1} < Q_D < 10^4$).

The efficiency with which thermal energy may be transformed into electrical energy is generally related to fluid temperature in a nonlinear manner. The response curves for transient thermal behavior may therefore only approximately be related to scaled electrical output. Efficiency usually increases with the absolute magnitude of the fluid production temperature and consequently the desire to maintain high temperatures, over time, may be crucial. The requirement of retaining production temperatures above a defined threshold suggests the desire to close off cooler zones with time. The feasibility of this option is controlled both by the surface-to-subsurface pumping arrangements and the hydraulically closed or interconnected nature of adjacent zones. For a colinear arrangement, however, the greatest thermal rebound is occasioned by halting circulation within the innermost zones. The proposed conceptual model offers the facility of optimizing power recovery subject to both economic and operational constraints applied to a realistic system.

The influence of the number of producing zones upon recovery temperature is apparent for

intermediate values of fluid throughput only. For dimensionless throughput values (Q_D) greater than 10^{-1} and less than 10^4 the effect is noticeable at large dimensionless times in the transient thermal record and, by inference, is retained in the steady case.

For optimal long term recovery it is desirable to retain dimensionless throughputs below 10^{-1} . The possibility of minimizing thermal depletion by reducing throughput, irrespective of the foregoing analysis, would appear an intuitive requirement in maintaining high effluent temperatures from the system. It is apparent that, for multiple production geometries, the relative thermal recovery is degraded with an increased number of zones. The relative recovery for one hundred zones is certainly degraded over that for ten, and a similar adjustment is anticipated with an increase in zone density above one hundred. This behavioral pattern is corroborated in the results for steady temperature outputs although, for dimensionless throughputs Q_D outside the range $10^{-1} < Q_D < 10^4$, the influence of the number of zones appears insignificant.

Acknowledgement—This material is a partial result of work supported by the National Science Foundation under Grant No. MSM-8708976.

REFERENCES

- Abé, H., Keer, L. M. and Mura, T. (1979) Theoretical study of hydraulically fractured penny-shaped cracks in hot dry rocks. *Int. J. num. analyt. meth. Geomechs.* **3**, 79–96.
- Baria, R., Green, A. S. P. and Jones, R. H. (1987) Anomalous seismic events observed at the CSM HDR Project. *Proceedings of the International Workshop on Forced Fluid Flow through Strong Fractured Rock Masses*, Commission of European Communities, EUR 11164/1, pp. 321–336 and *Int. J. Rock Mechs Min. Sci. Geomech. Abstr.* **26**, 3/4, 257–270.
- Bodvarsson, G. S. and Tsang, C. F. (1982) Injection thermal breakthrough in fractured geothermal reservoirs. *J. geophys. Res.* **87**, 1031–1048.
- Carslaw, H. S. and Jaeger J. C. (1959) *Conduction of Heat in Solids*, 2nd edn. Clarendon, Oxford.
- Elsworth, D. (1987) Thermal permeability enhancement of blocky rocks: plane and radial flow. *Proceedings of International Workshop on Forced Fluid Flow through Strong Fractured Rock Masses*, Commission of European Communities, EUR 11164/2, pp. 235–273 and *Int. J. Rock Mechs Min. Sci. Geomech. Abstr.* **26**, 3/4, 329–340.
- Elsworth, D. (1989a) Theory of thermal recovery from a spherically stimulated HDR reservoir. *J. geophys. Res.* **94**, 1927–1934.
- Elsworth, D. (1989b) A comparative evaluation of the parallel flow and spherical reservoir models of HDR geothermal systems. Internal Report, Waterloo Centre for Groundwater Research, pp. 1–17.
- Fehler, M. C. (1987) Stress control of seismicity patterns observed during hydraulic fracturing experiments at the Fenton Hill Hot Dry Rock Geothermal Energy Site, New Mexico. *Proceedings of the International Workshop on Forced Fluid Flow through Strong Fractured Rock Masses*, Commission of European Communities, EUR 11164/1, pp. 299–319 and *Int. J. Rock Mechs Min. Sci. Geomech. Abstr.* **26**, 3/4, 211–220.
- Gringarten, A. C. and Witherspoon, P. A. (1973) Extraction of heat from multiple fractured dry hot rock. *Geothermics* **2**, 119–122.
- Gringarten, A. C., Witherspoon, P. A. and Ohnishi, Y. (1975) Theory of heat extraction from fractured hot dry rock. *J. geophys. Res.* **80**, 1120–1124.
- Harlow, F. H. and Pracht, W. E. (1972) A theoretical study of geothermal energy extraction. *J. geophys. Res.* **77**, 7038.
- Lauwrier, H. A. (1955) The transport of heat in an oil layer caused by the injection of hot fluid. *Appl. scient. Res., Sect. (A)* **5**, 145.
- Murphy, H., Drake, R., Tester, J. and Zylvoski G. (1985) Economics of a conceptual 75MW hot dry rock geothermal electric power-station. *Geothermics* **14**, 459–474.
- Murphy, H. (1982) Hot dry rock reservoir development and testing in the U.S.A. *Proceedings of the 1st Japan-U.S. Seminar on Hydraulic Fracturing and Geothermal Energy*, Martinus-Nijhoff Publishers, pp. 33–58.
- Pine, R. J. and Batchelor, A. S. (1984) Downward migration of shearing in jointed rock during hydraulic injections. *Int. J. Rock Mechs Min. Sci. Geomech. Abstr.* **21**, 249–263.
- Smith, M. C. (1975) The Los Alamos Scientific Laboratory dry hot rock geothermal project (LASL Group Q-22). *Geothermics* **4**, 27–39.